ORIGINAL ARTICLE

Histopathological alteration in Zebrafish: Unravelling the Effects of Long-Term Copper Oxide Nanoparticle Exposure

Article history:
Received: 22-12-2023
Revised: 27-11-2024
Accepted: 28-11-2024

Himanshu Gupta[a], Mansee Thakur[b], Navami Dayal[c], Muskaan Singh[d], Jigesh Mehta[e], Ankit D. Oza[f], Chander Prakash[g]

Abstract: Copper Oxide nanoparticles (CuO-NPs) are widely used and they build up in the aquatic environment and can be harmful to aquatic life. Aquatic creatures are affected by CuO NPs, yet the consequences of these particles have not been well explored despite contentious toxicological results. Therefore, this study aimed to investigate the effects of chronic exposure to CuO-NPs on adult zebrafish. The study was carried out by conducting physicochemical characterization of commercially procured CuO-NPs using UV/Vis, ICP-OES spectroscopy, Transmission Electron Microscopy (TEM), X-ray diffraction (XRD), and Fourier Transform Infrared Spectroscopy(FTIR). Following characterization, adult zebrafish were chronically exposed to 0.5, 1, and 3 mg/l of CuO-NPs. Characterization revealed a heterogeneous population of nanoparticles in the size ranges of 10-50 nm. Oxidative stress indicators and functional markers were studied in addition to tissue histology. Chronic exposure to adult Fish at concentrations of 1 and 3 mg/l exhibited increased levels of stress compared to lower concentrations of 0.5 mg/l. Observations from histology showed that the extent of tissue damage and injuries increased with the concentration of CuO-NPs. In conclusion, chronic exposure to ≤50nm-sized CuO-NPs exhibited toxic repercussions in adult zebrafish.

Keywords: Copper oxide nanoparticles; TEM; FTIR; oxidative stress; histopathology; adult zebrafish; FET; Acridine orange.

[a] Dept. of Medical Biotechnology, MGM School of Biomedical Sciences, MGMIHS, Kamothe, Navi Mumbai 410209, India.

[b] Dept. of Medical Biotechnology, MGM School of Biomedical Sciences, MGMIHS, Kamothe, Navi Mumbai 410209, India.
Corresponding author: chander.mechengg@gmail.com

[c] School of Biotechnology and Bioinformatics, D Y Patil University, Navi Mumbai 400614, India.

[d] Dept. of Medical Biotechnology, MGM School of Biomedical Sciences, MGMIHS, Kamothe, Navi Mumbai 410209, India.

[e] Ganpat University, Ganpat Vidyanagar, Mehsana-Gandhinagar Highway, North Gujarat, 384012, India.

[f] University Centre of Research and Development, Chandigarh University, Mohali, Punjab, 140413, India.
Centre of Research Impact and Outcome, Chitkara University Institute of Engineering and Technology, Chitkara University, Rajpura-140401, Punjab, India.
School of Mechanical Engineering, Lovely Professional University, Phagwara, India.

[g] University Centre of Research and Development, Chandigarh University, Mohali, Punjab, 140413, India.
Corresponding author: mansibiotech79@gmail.com

INTRODUCTION

The increasing demand from consumers is driving a sharp increase in interest in nanotechnology. Diffusion, resistance to electricity, conductivity of electricity, strength, chemical reactivity, magnetism, and a broad spectrum of adaptive biological activity are amidst the distinctive chemical and physical attributes that distinguish these particles from their bulk counterparts (Mani *et al.*, 2019;Sahooli *et al.*, 2012). Commercial catalysts, chemical sensing instruments, therapeutic disinfection, and antimicrobials are just a few of the many possibilities for these nanoparticles. Additionally, they aid in the production of microelectronics and cosmetics (Katwal *et al.*, 2015). CuO-NPs' strong antibacterial and biocidal properties, which open up a variety of biomedical applications, have lately attracted a lot of attention (Nations *et al.*, 2015; Perreault *et al.*, 2012). Copper oxide is a metal-based semiconductor having distinct electrical, magnetic, and optical signals.

Among the many uses for them are the production of near-infrared filters, magnetic devices for storage, sensors, catalysis, semiconductors, and supercapacitors (Zhang *et al.*, 2014; Devi *et al.*, 2014; Dagher *et al.*, 2014). The biggest disadvantage of CuO-NPs, despite their widespread usage in many applications, is their potential for toxicity (Baek & An, 2011). CuO-NPS may be hazardous to both vertebrate and invertebrate cells, as well as to mammals. To assess the dangers of manufactured NMs, their ecotoxicological evaluations are crucial. The aquatic environment is particularly susceptible to exposure to artificial NMs because it serves as both a natural sink for pollutants and a natural route for their migration. (Bondarenko *et al.*, 2013). In aquatic creatures, CuO-NPs can cause acute and chronic toxicity. CuO-NPs are cytotoxic and genotoxic to lung epithelia, skin, peripheral blood, cancer cell lines, DNA changes and mutations, etc., according to in vitro investigations (Akhtar *et al.*, 2013). It has been found that CuO-NPs cause toxicity to the brain, liver, lungs, and kidneys (Zhang *et al.*, 2014). These nanoparticles can also induce oxidative stress, raise toxicity in human lung epithelial cells, and harm DNA and mitochondria. (Ruiz *et al.*, 2015).

Nanotoxicology research often uses zebrafish as a model since this teleost has 70% human genetic similarity. Nonetheless, there is now disagreement about the mechanism behind nanotoxicity, with several studies emphasizing different components (Devi *et al.*, 2014). External fertilization, a high number of spawns, translucent embryos, and quick development are all desirable characteristics of this organism (Dagher *et al.*, 2014). This model has various benefits, including fast growth and optical transparency, which allows for easy observation of phenotypic responses at fatal, acute, chronic, and sub-lethal toxicological endpoints.

Using mature zebrafish as animal models, the current research investigated the effects of CuO-NP exposure in vivo. The objective of the research was to investigate the sensitivity of CuO-NPs in the tissue of adult zebrafish. Oxidative stress indicators were assessed, including total protein content (PC), acetylcholinesterase enzyme activity (ACHE), catalyze activity (CAT), peroxidation of lipids (LPO), superoxide dismutase activity (SOD), and reactive oxygen species (ROS). Histological staining was performed to examine the tissue damage. Overall, the present work gave a clear view of CuO-NPs-induced tissue damage in adult zebrafish.

2. MATERIALS AND METHODOLOGY

2.1. Characterization of commercially purchased CuO-Nps

The CuO-NPs were commercially procured from Sigma Aldrich and ranged in size from less than 50 nm. The physical appearance of the nanoparticle was a powdery black substance. The sample was formulated as a solution before characterization experiments. 10 ml of Distilled water and 1 ml of CuO nanopowder were combined and the solution was thoroughly mixed with a magnetic stirrer for twenty minutes. An ultrasonicator was used for ten minutes to homogenise the mixture. The spectra were analyzed using the UV/Vis spectrophotometer at a scanning range of 200 to 900 nm. CuO nanoparticles were examined using transmission electron microscopy using an FEI Tecnai G2 F20 at 200 kV to determine their average size and shape. With the use of Vertex 80's infrared spectroscopy equipment (a main facility at IIT Mumbai), the presence or lack of functional groups at all was identified. CuK1.5405 radiation that has been nickel-filter was used to perform XRD on powdered material utilizing the RIGAKU XRD apparatus. Finally, inductively coupled plasma atomic emission spectrometry (ICP-AES) was used to determine the copper content in the CuO-NPs solution.

2.2. Zebrafish embryotoxicity

The ZEBCOG-Zebrafish facility, located at the Central Research Laboratory, MGMIHS, Navi Mumbai, was used to maintain adult zebrafish. The aquatic facility is equipped with GENDANIO automated recirculating Zebrafish housing system which was used to acclimatize the fish, which included a temperature of 28.5°C and a 10-hour light/dark cycle. The fish were fed with Frippak +300 (dry adult feed) twice a day and once with hatched live Artemia. Adult fish were bred, and eggs were collected. For the embryotoxicity study, a solution of varying concentrations of CuO-NPs was prepared by sonicating it for 30 minutes. The zebrafish embryos were exposed to 0.5, 1, and 3 mg/l of CuO-NPs and monitored for 6, 12, 24, 36, 48, 60, 72, 84, 96, 108, and 120 hours post-fertilization (hpf). It included three test groups and one control group with 10 eggs each. The experiments were performed in triplicate. The study was duly approved by the Institutional Animal Ethics Committee prior to starting

the experiments. Photographs were taken at various stages of the zebrafish embryos' development using an EVOS FL Auto microscope equipped with a digital camera. Developmental toxicity was assessed using factors such as the rate of embryonic development and the probability of both larvae and embryos surviving. Embryos treated with CuO-NPs also displayed pericardial oedema, a deformity similar to the anomalies observed in zebrafish embryos exposed to other toxins. Cellular death was assessed in live embryos to ascertain whether exposure to the test solution caused cellular apoptosis in the zebrafish embryo. Using Acridine Orange (AO) staining of larvae exposed to test amounts at 96 hpf, cellular apoptosis was examined. The embryos were removed 96 hours post fertilization, cleaned in phosphate-buffered saline, placed in Eppendorf tubes, and left to be exposed to 10 µg/mL doses of AO for 30 minutes at room temperature. Before visualization, the embryos were repeatedly washed in phosphate-buffered saline. Using carboxymethyl cellulose (CMC) to immobilize the larvae, the EVOS FL AUTO Imaging microscope was used to monitor the larvae under a GFP filter (520nm emission).

2.3. Adult zebrafish toxicity

All studies on adult zebrafish were performed following the OECD 209 and 329 guidelines. The MGMIHS Institutional Animal Care Committee gave its approval to the project. The mature zebrafish were split into four groups at random, consisting of seven fish each, and were exposed to the following treatments for thirty days in each group:

Group 1: Controls maintained in D/W.
Group 2: Water distillate containing 0.5 mg/l CuO-NPs
Group 3: Water distillate containing 1 mg/l CuO-NPs
Group 4: Water distillate containing 3 mg/l CuO-NPs

The treatment and control groups were given the appropriate amounts of fresh CuO-NPs along with water distillate renewed every 24 hours. Each group received the same feed throughout the study. Continuous oxygenation was provided to the fish. Following the final day of treatment, fish were immersed in tricaine methane sulfonate (200–300 mg/l) for about 10 minutes or till the opercular movement stopped, after which the fish were immersed in cold water. Oxidative stress measurements and histological examinations were performed on the test and control groups.

2.4. Protein content

Protein content was estimated (Dagher *et al*., 2014). The technique for estimating total protein content used bovine serum albumin (BSA) as a standard. Distilled water was used to dilute 0.1 ml of the tissue homogenate to achieve a final concentration of 1 ml. To the mixture, an additional 5 milliliters of caustic copper reagent were added. After thoroughly mixing, the mixture was allowed to sit at room temperature for ten minutes without being disturbed. 0.5 mL of a 1N Folin-Ciocalteu phenol solution was subsequently added to this tube and it was vigorously stirred. After that, the combination was left to incubate at room temperature for a full twenty minutes. The brightness of the blue color was assessed at a wavelength of 620 nm using a blank reagent that included all necessary components except for the tissue homogenate. Typically, the concentration of the protein is denoted in milligrams (mg) per tissue.

2.5. Acetylcholinesterase enzyme activity (ACHE)

Using the Ellman *et al.* technique, the ACHE activity was observed (Aksnes *et al*., 2019). 50µl of the sample was added to a reaction mixture containing 100µl of 10mM 5,5′-Dithiobis (2-nitrobenzoic acid) and 50µl of 1M potassium phosphate buffer to conduct the test. The addition of 20 mL of a 25 mM solution of acetylthiocholine iodide initiated the reaction. The whole reaction was thereafter incubated at a temperature of 37 °C for 10 minutes. The yellow hue was measured using spectrophotometry at an emission wavelength of 412 nm, with the sample substituted with a blank that contained 50 µl of distilled water. Thiocholine hydrolysis was used to measure AChE activity, and the findings were expressed as units per milligram of protein.

2.6. Oxidative stress markers

2.6.1. Reactive oxygen species (ROS)

The quantity of ROS was measured using the Beauchamp and Fridovich method (Beauchamp

& Fridovich, 1971). One common technique to assess superoxide generation is nitroblue tetrazolium (NBT) reduction. Ten milligrams of tissue were homogenized using one ml of Hank's balancing salt solution (HBSS). Each test sample received 0.5 ml of NBT-HBSS, and it was then incubated at 37 °C for eight hours. The test samples were then centrifuged at 1,000 rpm for 10 minutes at 4 degrees Celsius. After that, the pellet was given three washes, each using 200 µl of methanol. The pellet was then dissolved in a mixture of 1 milliliter of 2M KOH and 1 milliliter of DMSO. After that, measurements of optical density (OD) at 630 nm were made and compared to a reference curve made using NBT. The generation of reactive oxygen species, or ROS, is expressed as a percentage of the control condition.

2.6.2. Lipid peroxidation (LPO)

LPO was calculated using the protocol given by Devasagayam and Tarachand (Devasagayam & Tarachand, 1987). This test involved a total of 0.9 ml of reactant mixture, which included 0.5 ml of 0.15M Tris-HCl buffer (pH 7.4), 0.15 ml of 10 M KH2PO4, 0.1 ml of tissue homogenate, and 0.25 ml of distilled water. For 20 minutes, the tubes were vigorously shaken in an incubator set at 37 °C. The reaction was stopped by adding 1 ml of 10% trichloroacetic acid (TCA). Thiobarbituric acid, a solution containing 0.75 ml of 0.67% TBA, was added after the tubes were vigorously shaken. After that, for twenty minutes, they were submerged in water that was boiling. We measured the color at 532 nm after the tubes had been centrifuged. Nanograms of malondialdehyde (MDA) per milligram of protein is the unit of expression used to describe the sample compounds.

2.6.3. Superoxide Dismutase (SOD)

Marklund's technique (Marklund & Marklund, 1974) was followed to assess SOD levels. The following volumes were mixed: 0.15 ml of chloroform, 0.25 ml of cold 100% ethanol, and 0.5 ml of material extract. After stirring the mixture for 15 minutes in a mechanical shaker, it was spun down at 13,000 rpm for another 15 minutes that followed. Use of half a milliliter of the supernatant as a test was performed. The auto-oxidation reaction mixture consisted of 2 mL of Tris-HCl buffer with a pH of 8.2, 0.5 mL of a 2-mL Pyrogallol solution, and 2 mL of water. Initially, for three minutes, we monitored the rate of pyrogallol auto-oxidation. Each measurement was taken at a 1-minute interval. This process was thought to be fully auto-oxidative. The enzyme test mixture included 2 milliliters of Tri-HCl buffer (pH 8.2), half a milliliter of a 2 millimolar Pyrogallol solution, half a milliliter of the enzyme mix, and enough water to make the final volume 4.5 milliliters. For the blank, 2.0 ml of a pH 8.2 Tris-HCl buffer and 2.5 ml of distilled water were used. After adding the enzyme, the rate of inhibition of pyrogallol auto-oxidation was measured. Enzyme activity was measured in units per milligram of protein.

2.6.4. Catalase activity

The method outlined (Turan, 2021) was used to calculate the catalase (CAT) activity. 0.5 ml of hydrogen peroxide (H2O2) and 1 ml of phosphate buffer (pH 7.0) were added to 1 ml of homogenate. To finish the reaction, 2 milliliters of dichromate acetic acid solution were added at 0, 30, and 60 seconds. The mixture was then placed in a bath of boiling water for 10 minutes. To determine the protein content, the absorbance at 590 nm was measured. Histopathology:

After exposing the samples to CuO-NPs continuously for 28 days, a histological examination was performed. The fish were put to sleep in cold water and then dissected to extract vital organs such as the liver, intestines, brain, pancreas, and muscle. The organs were left to fix in 10% formalin at room temperature for a full day. The paraffin wax was used to implant the dried fixed tissue. A Leica RM255 microtome was used to cut 5 µm serial cross sections, which were subsequently stained with both eosin and hematoxylin (H & E). The samples were inspected using an Olympus Magnus light microscope (Model No. 11F589) (Menke *et al.*, 2011).

2.7. Statistical analysis

From a statistical standpoint, every experiment was carried out in triplicate. Plotted using Python 3.12, packages of Pandas and Matplotlib, were used for analyzing the data. The data were shown as the average plus or minus the standard deviation. The data was examined for normality and unity. When $p<0.05$, we were said to have very significant differences.

3. RESULTS AND DISCUSSION

3.1. Characterization of commercially purchased CuO NPs

3.1.1. UV-Vis absorption spectroscopy

Using a BioTek Epoch 2 microplate spectrophotometer, UV-Vis absorption was carried out at the MGM Central Research Laboratory as shown in Figure 1. Based on the absorption peak at 230 nm (λmax), the study verified the existence of CuO-NPs. The spectroscopic readings were repeated for a week and fortnight, to check the stability and to confirm the nanoparticles' long-term endurance. Over three months, it was discovered that the nanoparticles were stable. Similar results were achieved using a 200-600 nm range, and 398 and 527 nm were confirmed to be the peaks (A Brief Review," 2016).

Well	Mean Min OD [Spectrum]	W at Mean Min OD [Spectrum]	Mean Max OD [Spectrum]	W at Mean Max OD [Spectrum]
F8	0.063	900	3.571	230

Figure 1. UV-Vis absorption spectra of commercially purchased CuO-NPs revealing λmax at 230nm.

3.1.2. Fourier transmission electron microscopy

The FTIR measurements of the commercially purchased CuO-NPs are given in Figure 2, which was performed at the central facility of SAIFat IIT-Mumbai using Vertex 80. FTIR analysis helped in identifying the presence of functional groups. Fig. 2 shows that the stretching vibrations of aliphatic C-H bonds are reflected by the prominent peaks at 3434, 1707, 1464, and 1229 cm^{-1}, respectively. Copper oxide nanoparticles' Cu (I)-O vibrations are corresponding to the 610 and 505 cm1 peaks, respectively. The peaks and matching bonds in O-H, =C-H, C-C bonds, etc. showed similar findings (Kadam *et al.*, 2020).

3.1.3. Inductively coupled plasma atomic emission spectroscopy

ICP-AES, an outsourced elemental analysis tool, was used to find an 87.6% Cu concentration in the NPs.

3.1.4. X-ray diffraction analysis

The commercially obtained CuO-NPs underwent XRD analysis using RIGAKU, and the results showed that the specimen had a structure that was crystalline since it had distinct Bragg peaks (Figure 3). Two primary peaks were seen in the XRD patterns at 2θ=35.6° and 2θ=38.82°, which are attributed to the (−111) and (111) reflections of the CuO phase. These reflections are comparable to those reported (Etefagh *et al.*, 2017). The position 2θ of the Bragg peak is governed by Bragg's law for X-ray diffraction. The sharp peaks suggested that CuO nanoparticles had a fine crystal structure with high purity. Sharp Bragg peaks (δ- function) indicate particles having macroscopic size. The Bragg peaks, however, broaden as the particle size decreases (Marulasiddeshi *et al.*, 2022). The presence of broad Bragg peaks is consistent with the fact that samples consist of nanoparticles (Ahamed *et al.*, 2014).

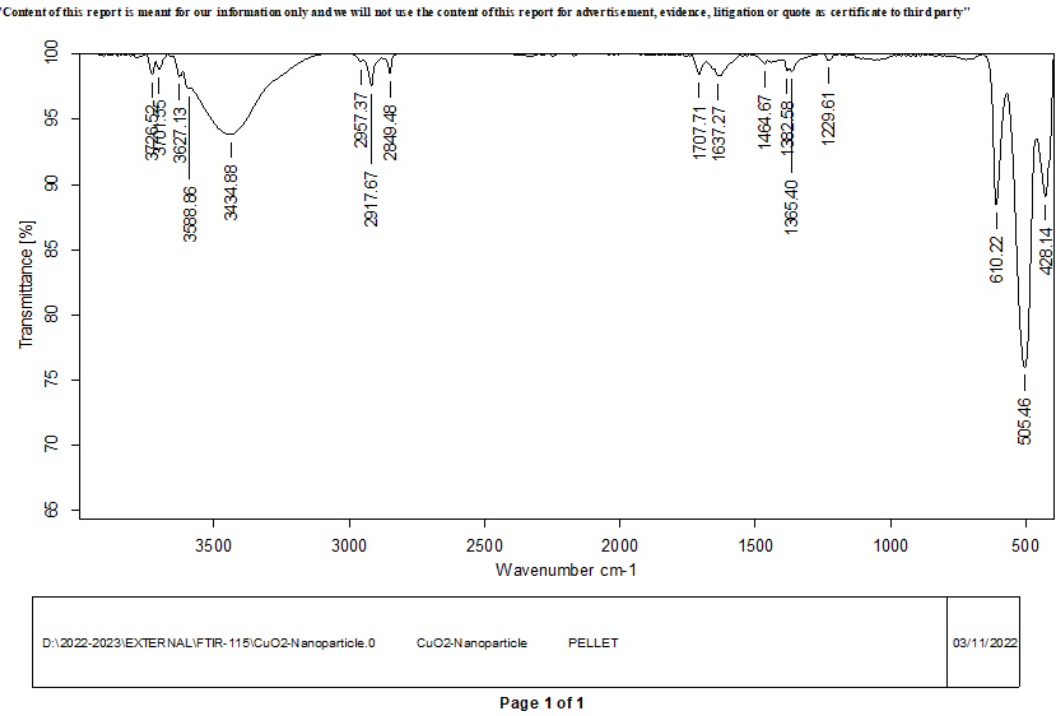

Figure 2. Strong peaks found in the FTIR spectra of commercially obtained CuO-NPs at 3434, 1707, 1464, and 1229 cm^{-1}, respectively. These correspond to the OH, C=C, C–O, and aliphatic C–H stretching vibrations. The vibration of CuO-NPs is associated with Cu (I)–O at peaks of 610 and 505 cm^{-1}.

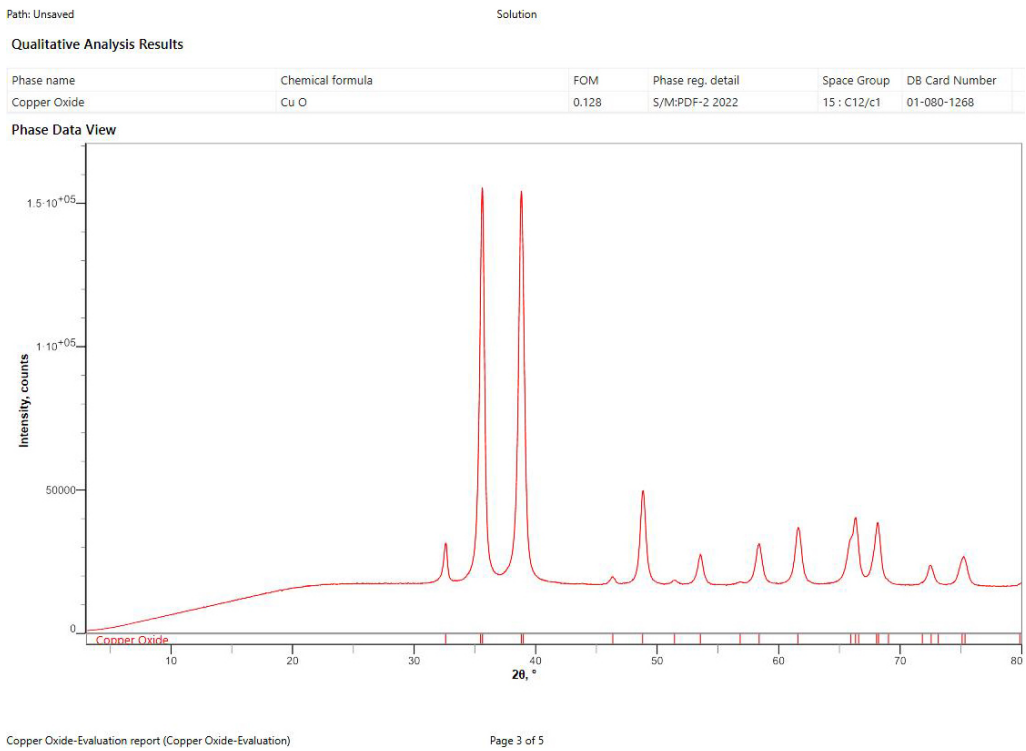

Figure 3. Commercially acquired CuO NPs' XRD pattern showed two primary peaks, representing the CuO phase, at $2\theta=35.6°$ and $2\theta=38.82°$. The wide Bragg peaks are also discernible, which is consistent with the samples' nanoparticle composition.

3.1.5. Transmission electron microscopy

The CuO nanoparticles that were purchased commercially were micrographed using a transmission electron microscope, FEI Tecnai G2, F30 (Bin Mobarak *et al.*, 2022). The micrographs revealed that the nanoparticles exhibited polydispersity, ie. their shape was more or less uniform. However, the particle sizes varied between 13 and 100 nm, with the average diameter of the nanoparticles being less than 50 nm (Figure 4). Some visible aggregation was also found. The results of the TEM imaging of the commercially bought CuO-NPs were in accordance (Naz *et al.*, 2019).

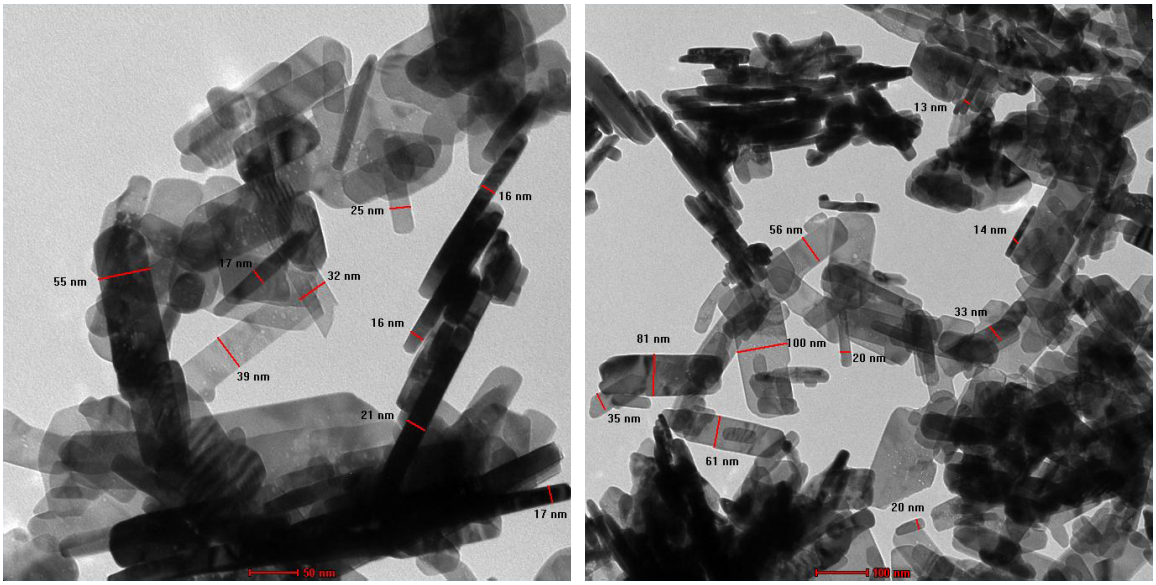

Figure 4. The commercially obtained CuO NPs showed a TEM micrograph of obvious aggregation. The particles were evenly formed, polydisperse, and ranged in size from 13 to 100 nm, with an average diameter of less than 50 nm.

3.2. Fish embryo toxicity

Zebrafish embryos were used to test the effects of CuO-NPs at concentrations of 0.5, 1, and 3 mg/L. The CuO-NPs had a negative impact on the embryos. Hatching rates were normal; however, at 72 hpf, mild oedema was visible in embryos for all concentrations. An increase in the death rates of the embryos was observed at 108 hpf and 120 hpf as the concentration increased. Normal development was observed in the embryos of the control group at 24-120 hpf. According to the findings of the study, CuO-NPs were unable to penetrate the tissues of the zebrafish embryos and larvae. However, they did cause an increase in the mortality rate, a delay in hatching, and a drop in the heartbeat rate as seen in Table 1 and Figure 5. In addition, CuO-NPs were responsible for a variety of anomalies manifesting themselves in groups that contained smaller amounts (Aksakal & Ciltas, 2019).

The preceding figure makes it very clear that the degree of damage and toxicity caused by Np's increases as their concentration increases, negatively impacting the viability of larvae and embryos. This data makes it clear that the concentration of less than 1 mg/ml may correspond to the lower limit of detection (LC 50) for copper oxide nanoparticles smaller than 50 nm. The test group displayed bent notochord at 120 hpf, as indicated by arrows, pericardial edema, and embryonic death at 108 and 120 hpf.

3.3. Histopathology results

After chronic exposure to CuO-NPs, various deleterious effects were observed in the architecture of major organs of adult zebrafish as studied using histopathological analysis (Yang *et al.*, 2021).

3.3.1. Liver

Figure 6 shows the histological alterations in the liver of zebrafish subjected to CuO-Np's., hepatic parenchyma exhibited mild to severe necrosis, accompanied by disorganization of the biliary channels, at concentrations of 0.5, 1, and 3mg/l.

Physiological effects	24hpf				48hpf				72hpf				96hpf			
	Control	0.5mg/l	1mg/l	3mg/l	Control	0.5mg/l	1mg/l	3mg/l	Control	0.5mg/l	1mg/l	3mg/l	Control	0.5mg/l	1mg/l	3mg/l
% viability	100%				100%				100%			60%	100%		60%	20%
Motility	+	+	+	+	+	+	+	+	+	+	+	↓	+	+	↓	↓
Hatching	–	–	–	–	–	–	–	–	+	+	+	↓	–	–	–	–
Heart beat	–	–	–	–	+	+	+	+	+	+	↓	↓	+	+	dead	dead
Edema Formation	–	–	–	–	–	–	–	–	–	–	–	+	–	–	+	+
Tail Deformity	–	–	–	–	–	–	–	–	–	–	–	–	–	–	–	–

Table 1. Endpoints recorded after being exposed to the three NP concentrations.

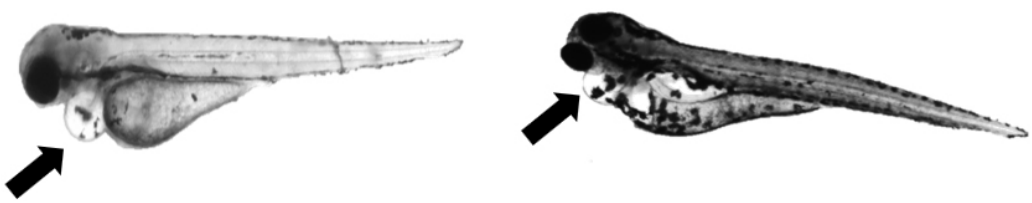

Figure 5. Block arrows indicate the development of edema following exposure to 1 and 3 mg/l of CuO NPs.

Vacuoles of different shapes and sizes were detected in the cytoplasm of hepatocytes. The administration of a 3mg/l dosage resulted in the presence of hepatocytes with pleomorphic nuclei exhibiting diverse sizes and levels of activity (Carvalho *et al.*, 2017). In addition, the necrotic hepatocytes were characterized by larger cells, pyknotic nuclei, and pale cytoplasm. Observations revealed hepatocytes with pleomorphic nuclei exhibiting varying sizes and levels of activity, including both euchromatic and heterochromatic regions. The scale bars measure 50 micrometers.

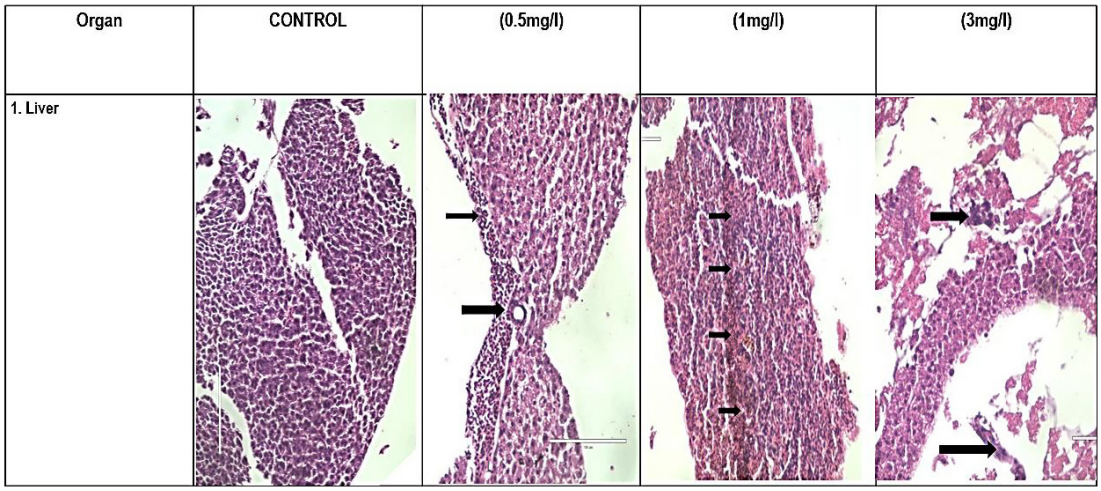

Figure 6. Under an optical microscope with a 100X magnification, histological sections of the liver of zebrafish revealed vacuoles of different forms in addition to mild to moderate necrosis of the hepatic parenchyma. The 3 mg/l group's nuclei were pleomorphic.

3.3.2. Intestine

Zebrafish treated with CuO-Nps showed histological alterations in their intestines, as seen in Figure 7. This observation suggests that the fish may have evolved a defensive mechanism against the toxicity since no fish died after exposure. Toxic chemical exposure damages the mucosa of the intestine and inhibits cellular growth in intestinal tissue, disrupting the physiology of the intestinal

tissue as shown by histological alterations. Inflammation of the lamina propria is a common characteristic of damage to the intestines brought on by toxic chemicals (Win-Shwe & Fujimaki, 2011). The infiltration of leukocytes, mostly neutrophils, is a characteristic of inflammation. Pathological sections of the gut revealed the presence of additional zebrafish inflammatory cells, including monocytes and lymphocytes. Hyperplasia of goblet cells was seen in the groups receiving 3mg/l. These results further support the increased hyperemia by demonstrating the presence of white blood cells in the tissue due to inflammation (Yang *et al.*, 2021; Carvalho *et al.*, 2017).

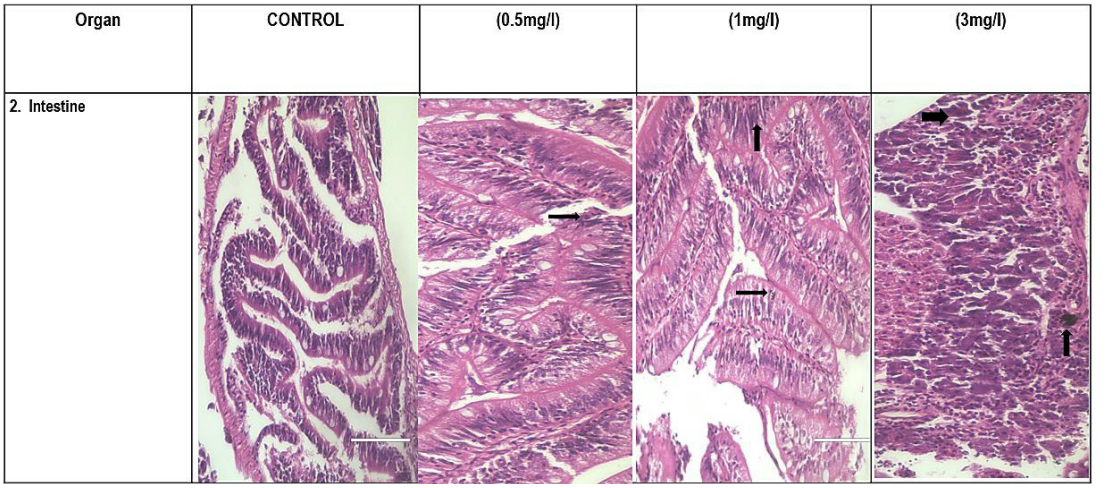

Figure 7. Under an optical microscope set to 100X magnification, histological slices of the zebrafish gut revealed the presence of inflammatory cells, denoted by block arrows.

3.3.3. Brain

Previous studies on the neurotoxicity of nanoparticles have shown that these particles may enter the brain and induce neurodegeneration (Carvalho *et al.*, 2017). Prospects of nanoparticles on brain-targeted drug delivery also evaluated nanoparticle-induced neurotoxicity using the zebrafish model. As evident from the images in Figure 8, there is damage to the ciliated columnar epithelium at the higher concentrations of 1 and 3mg/l.

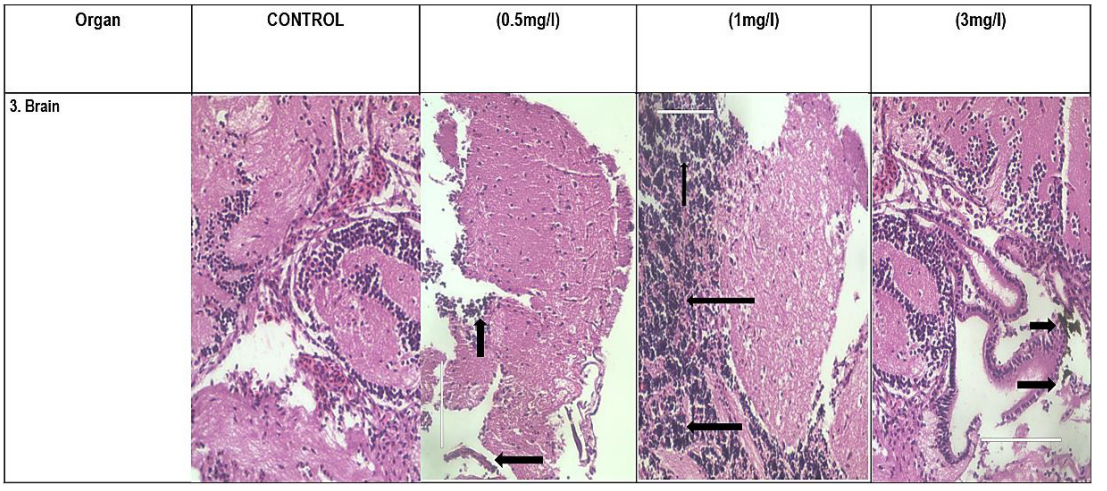

Figure 8. Under an optical microscope with 100X magnification, histological sections of the zebrafish brain demonstrate damage to the ciliated columnar epithelium at greater doses of 1 and 3 mg/l.

3.3.4. Pancreas

In most tissue sections, the pancreas segments of the group receiving treatment had modest degenerative alterations in the cellular components of the pancreatic islets, with many cells exhibiting pyknotic nuclei and irregular cytoplasmic vacuolation as shown in Figure 9. Dark exocrine pancreas and lighter endocrine pancreas are visible in the control sections in comparison to the treated groups indicated by arrows.

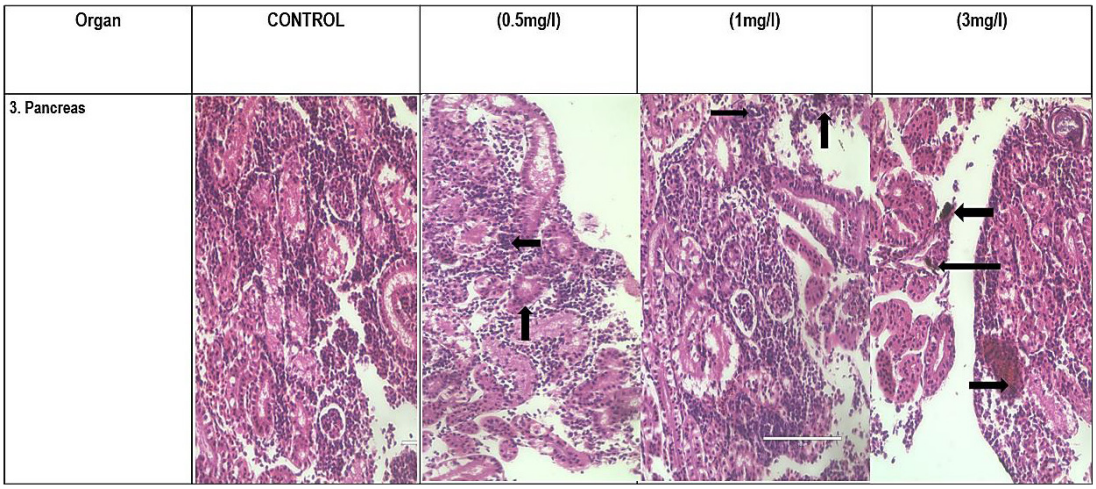

Figure 9. Under an optical microscope with a 100X magnification, histological slices of zebrafish pancreas reveal small degenerative alterations in the pancreatic islets as well as a large number of cells with pyknotic nuclei and irregular cytoplasmic vacuolation. Block arrows in the control areas show that the exocrine pancreas is darker and the endocrine pancreas is lighter than in the treatment groups.

3.3.5. Muscle

The control group's skeletal muscle had normal skeletal muscle histoarchitecture, whereas the groups treated with 1 mg/l CuO-NPs displayed modest perimysial inflammation and fibrillary degeneration, as shown by the arrows in Figure 10. Vacuolar degeneration accompanied by atrophy was seen in the groups treated with 3 mg/l CuO-NPs. A 3 mg/l exposure to CuO-NPs causes muscle toxicity, as shown by changes in the tissue architecture. According to related research, adult zebrafish had muscle degeneration as a result of persistent exposure to CuO-NPs that produced muscle toxicity (Win-Shwe & Fujimaki, 2011; Samim & Vaseem, 2023).

3.4. ACHE, Protein Content and Oxidative Stress Markers

Our findings showed that the main internal structures of zebrafish were seriously harmed by CuO-NP concentrations of 0.5,1 and 3 mg/l. This work is among the first to show that CuO-NPs negatively impact zebrafish's main organs, including stress indicators.

Analysis was done on the outcomes of oxidative stress indicators such as ROS, SOD, LPO, and CAT, as well as functional markers such as Acetylcholinesterase (ACHE), Protein content (PC), and others. The fall in antioxidant levels was accompanied by a notable rise in oxidants, indicating that the CuO-NP-induced free radicals were too strong for antioxidant enzymes to neutralize. The overall protein content of the muscle tissue was significantly higher in the 0.5 mg/l, 1 mg/l, and 3 mg/l groups than in the control. However, ACHE activity was significantly lower in CuO-NP treated groups than in control groups. The oxidative stress markers in adult zebrafish were investigated after their exposure to CuO-NPs (Figure 11). When comparing the fish exposed to CuO-NPs to the control, a consistent rise in LPO (lipid peroxidation) and ROS (reactive oxygen species) was observed. The fish treated with CuO-NPs showed a sharp decrease in SOD (superoxide dismutase) levels and a rise in CAT (catalyze activity). Figure 11 shows how the indicators changed dramatically in a dose-dependent manner, indicating that those receiving treatment had higher levels of oxidative stress. All other results were consistent (Mani *et al.*, 2019), except the CAT result, which was shown to have risen.

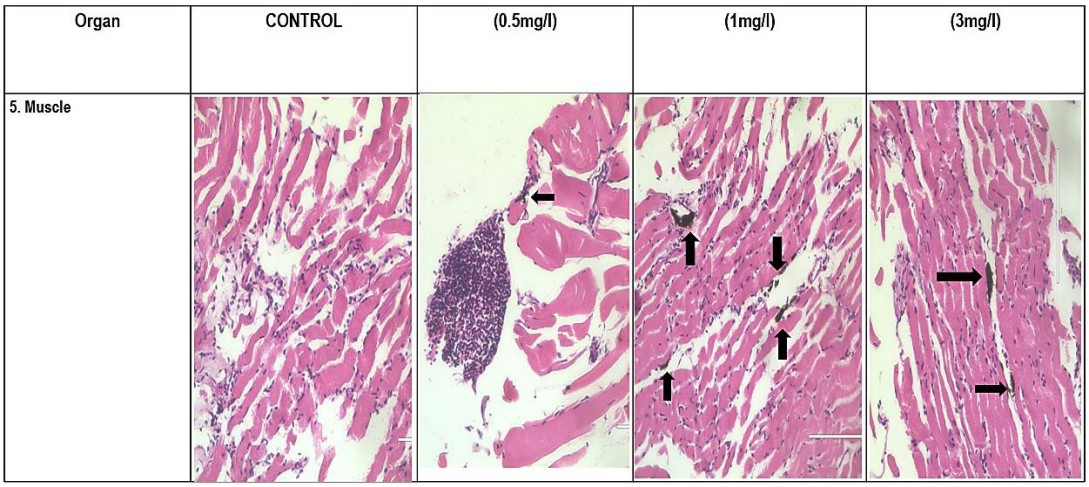

Figure 10. Under an optical microscope with 100X magnification, histological slices of zebrafish skeletal muscle were examined. The control group displayed normal skeletal muscle histo-architecture, while the treatment groups displayed minor perimysial inflammation and fibrillary degeneration, as indicated by arrows. Groups treated with 3 mg/l CuO-NPs exhibited atrophy along with degeneration and vacuolar degeneration, as illustrated by arrows.

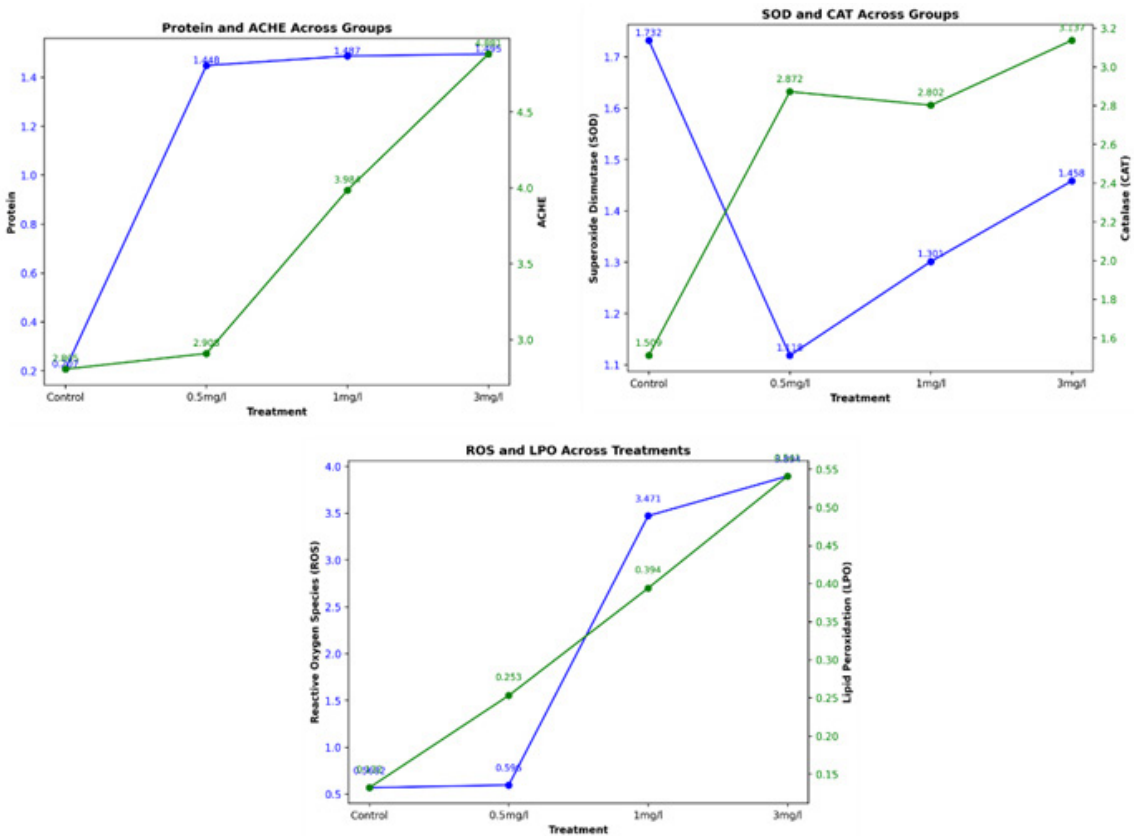

Figure 11. Graphical representation of Protein content & ACHE activity, oxidative stress markers- SOD & CAT and ROS & LPO of control and CuO-NPs treated groups Plotted using python 3.12, packages used are pandas and matplotlib

4. CONCLUSION

Zebrafish are now used in toxicology as a highly developed vertebrate model. This model has been widely used for toxicological evaluation of nanoparticles for over a decade due to its superior efficiency, low cost, and ease of implementation. The concentration of environmental contaminants in water may be determined with the use of this easy to maintain model system. The zebrafish, with the help of cutting-edge technology, may soon replace the existing mammalian models in the toxicity assessment of nanomaterials.

The present study used commercially purchased CuO-NPs. Characterization using TEM, XRD, FTIR and UV/Vis Spectroscopy revealed the nature of these particles to be heterogenous and the average diameter to be within 50nm. These nanoparticles were used to assess Fish embryo toxicity and study the effect of chronic exposure on adult zebrafish. The current study showed that CuO-NPs are harmful to the major organs of adult zebrafish in addition to exhibiting embryo toxicity. The liver, brain, and intestines all revealed signs of injury on histopathology examination. When compared to the control groups, both oxidative stress and functional indicators were found to be significantly elevated. Furthermore, there was an increase in protein content in the treated groups, indicating increased oxidative stress and toxicity that was dose-dependent. The majority of the documented impacts are caused by oxidative stress, which is influenced by the CuO-NPs' size, shape, and solubility. More oxidative stress resulted in the generation of free radicals. Free radicals were produced as a result of the increased oxidative stress, and the body's antioxidant defenses had difficulty neutralizing them. As a result, morphological examinations revealed tissue damage. The current findings will help to illuminate the poorly understood mechanism of muscle poisoning caused due to CuO-NPs. This research is also important for limiting the harm caused by CuO-NPs to aquatic life in the environment.

Author Contributions

H. G., M. T., concept, writing-original draft preparation, investigation, resources, data curation; N. D, M. S. writing-review and editing, methodology, formal analysis; H. T. & M. T. conceptualization, A. D. O & J. P. M., supervision, project administration, all authors have read and agreed to the published version of the manuscript.

Funding

Nil

Acknowledgments

Special thanks to ZEBCOG-Zebrafish Laboratory, CRL Lab, MGMSBS, MGMIHS, for providing the infrastructure.

Conflicts of Interest

The authors declare no conflict of interest. ♦

REFERENCES

A brief review on synthesis and characterization of copper oxide nanoparticles and its applications. (2016). *Journal of Bioelectronics and Nanotechnology, 1*(1). https://doi.org/10.13188/2475-224x.1000003

Ahamed, M., Alhadlaq, H. A., Khan, M. A., Karuppiah, P., & Al-Dhabi, N. A. (2014). undefined. *Journal of Nanomaterials, 2014*(1). https://doi.org/10.1155/2014/637858

Akhtar, M. J., Kumar, S., Alhadlaq, H. A., Alrokayan, S. A., Abu-Salah, K. M., & Ahamed, M. (2013). Dose-dependent genotoxicity of copper oxide nanoparticles stimulated by reactive oxygen species in human lung epithelial cells. *Toxicology and Industrial Health, 32*(5), 809-821. https://doi.org/10.1177/0748233713511512

Aksakal, F. I., & Ciltas, A. (2019). Impact of copper oxide nanoparticles (CuO NPs) exposure on embryo development and expression of genes related to the innate immune system of zebrafish (Danio rerio). *Comparative Biochemistry and Physiology Part C: Toxicology & Pharmacology, 223*, 78-87. https://doi.org/10.1016/j.cbpc.2019.05.016

Aksnes, D. W., Langfeldt, L., & Wouters, P. (2019). Citations, citation indicators, and research quality: An overview of basic concepts and theories. *Sage Open, 9*(1). https://doi.org/10.1177/2158244019829575

Baek, Y., & An, Y. (2011). Microbial toxicity of metal oxide nanoparticles (CuO, NIO, ZnO, and Sb2O3) to escherichia coli, bacillus subtilis, and streptococcus aureus. *Science of The Total Environment, 409*(8), 1603-1608. https://doi.org/10.1016/j.scitotenv.2011.01.014

https://doi.org/10.37819/nanofab.9.2030

Beauchamp, C., & Fridovich, I. (1971). Superoxide dismutase: Improved assays and an assay applicable to acrylamide gels. *Analytical Biochemistry, 44*(1), 276-287. https://doi.org/10.1016/0003-2697(71)90370-8

Bin Mobarak, M., Hossain, M. S., Chowdhury, F., & Ahmed, S. (2022). Synthesis and characterization of CuO nanoparticles utilizing waste fish scale and exploitation of XRD peak profile analysis for approximating the structural parameters. *Arabian Journal of Chemistry, 15*(10), 104117. https://doi.org/10.1016/j.arabjc.2022.104117

Bondarenko, O., Juganson, K., Ivask, A., Kasemets, K., Mortimer, M., & Kahru, A. (2013). Toxicity of Ag, CuO and ZnO nanoparticles to selected environmentally relevant test organisms and mammalian cells in vitro: A critical review. *Archives of Toxicology, 87*(7), 1181-1200. https://doi.org/10.1007/s00204-013-1079-4

Carvalho, J. C., Keita, H., Santana, G. R., De Souza, G. C., Dos Santos, I. V., Amado, J. R., Kourouma, A., Prada, A. L., De Oliveira Carvalho, H., & Silva, M. L. (2017). Effects of Bothrops alternatus venom in zebrafish: A histopathological study. *Inflammopharmacology, 26*(1), 273-284. https://doi.org/10.1007/s10787-017-0362-z

Dagher, S., Haik, Y., Ayesh, A. I., & Tit, N. (2014). Synthesis and optical properties of colloidal CuO nanoparticles. *Journal of Luminescence, 151*, 149-154. https://doi.org/10.1016/j.jlumin.2014.02.015

Devasagayam, T. P., & Tarachand, U. (1987). Decreased lipid peroxidation in the rat kidney during gestation. *Biochemical and Biophysical Research Communications, 145*(1), 134-138. https://doi.org/10.1016/0006-291x(87)91297-6

Devi, A. B., Moirangthem, D. S., Talukdar, N. C., Devi, M. D., Singh, N. R., & Luwang, M. N. (2014). Novel synthesis and characterization of CuO nanomaterials: Biological applications. *Chinese Chemical Letters, 25*(12), 1615-1619. https://doi.org/10.1016/j.cclet.2014.07.014

Etefagh, R., Rozati, S., Azhir, E., Shahtahmasebi, N., & Hosseini, A. (2017). Synthesis and antimicrobial properties of ZnO/PVA, CuO/PVA, and TiO2/PVA nanocomposites. *Scientia Iranica, 24*(3), 1717-1723. https://doi.org/10.24200/sci.2017.4147

Kadam, J., Dhawal, P., Barve, S., & Kakodkar, S. (2020). Green synthesis of silver nanoparticles using cauliflower waste and their multifaceted applications in photocatalytic degradation of methylene blue dye and Hg2+ biosensing. *SN Applied Sciences, 2*(4). https://doi.org/10.1007/s42452-020-2543-4

Katwal, R., Kaur, H., Sharma, G., Naushad, M., & Pathania, D. (2015). Electrochemical synthesized copper oxide nanoparticles for enhanced photocatalytic and antimicrobial activity. *Journal of Industrial and Engineering Chemistry, 31*, 173-184. https://doi.org/10.1016/j.jiec.2015.06.021

Lowry, O., Rosebrough, N., Farr, A. L., & Randall, R. (1951). Protein measurement with the folin phenol reagent. *Journal of Biological Chemistry, 193*(1), 265-275. https://doi.org/10.1016/s0021-9258(19)52451-6

Mani, R., Balasubramanian, S., Raghunath, A., & Perumal, E. (2019). Chronic exposure to copper oxide nanoparticles causes muscle toxicity in adult zebrafish. *Environmental Science and Pollution Research, 27*(22), 27358-27369. https://doi.org/10.1007/s11356-019-06095-w

Marklund, S., & Marklund, G. (1974). Involvement of the superoxide anion radical in the Autoxidation of pyrogallol and a convenient assay for superoxide Dismutase. *European Journal of Biochemistry, 47*(3), 469-474. https://doi.org/10.1111/j.1432-1033.1974.tb03714.x

Marulasiddeshi, H. B., Kanti, P. K., Jamei, M., Prakash, S. B., Sridhara, S. N., & Said, Z. (2022). Experimental study on the thermal properties of al $_2$ O $_3$ -cuo /water hybrid nanofluids: Development of an artificial intelligence model. *International Journal of Energy Research, 46*(15), 21066-21083. https://doi.org/10.1002/er.8739

Menke, A. L., Spitsbergen, J. M., Wolterbeek, A. P., & Woutersen, R. A. (2011). Normal anatomy and histology of the adult Zebrafish. *Toxicologic Pathology, 39*(5), 759-775. https://doi.org/10.1177/0192623311409597

Nations, S., Long, M., Wages, M., Maul, J. D., Theodorakis, C. W., & Cobb, G. P. (2015). Subchronic and chronic developmental effects of copper oxide (CuO) nanoparticles on xenopus laevis. *Chemosphere, 135*, 166-174. https://doi.org/10.1016/j.chemosphere.2015.03.078

Naz, S., Gul, A., & Zia, M. (2019). Toxicity of copper oxide nanoparticles: A review study. *IET Nanobiotechnology, 14*(1), 1-13. https://doi.org/10.1049/iet-nbt.2019.0176

Perreault, F., Melegari, S. P., Da Costa, C. H., De Oliveira Franco Rossetto, A. L., Popovic, R., & Matias, W. G. (2012). Genotoxic effects of copper

oxide nanoparticles in Neuro 2a cell cultures. *Science of The Total Environment, 441*, 117-124. https://doi.org/10.1016/j.scitotenv.2012.09.065

Ruiz, P., Katsumiti, A., Nieto, J. A., Bori, J., Jimeno-Romero, A., Reip, P., Arostegui, I., Orbea, A., & Cajaraville, M. P. (2015). Short-term effects on antioxidant enzymes and long-term genotoxic and carcinogenic potential of CuO nanoparticles compared to bulk CuO and Ionic copper in mussels mytilus galloprovincialis. *Marine Environmental Research, 111*, 107-120. https://doi.org/10.1016/j.marenvres.2015.07.018

Sahooli, M., Sabbaghi, S., & Saboori, R. (2012). Synthesis and characterization of mono sized CuO nanoparticles. *Materials Letters, 81*, 169-172. https://doi.org/10.1016/j.matlet.2012.04.148

Samim, A. R., & Vaseem, H. (2023). Exposure to nickel oxide nanoparticles induces alterations in antioxidant system, metabolic enzymes and nutritional composition in muscles of Heteropneustes fossilis. *Bulletin of Environmental Contamination and Toxicology, 110*(4). https://doi.org/10.1007/s00128-023-03714-8

Turan, V. (2021). Calcite in combination with olive pulp biochar reduces Ni mobility in soil and its distribution in chili plant. *International Journal of Phytoremediation, 24*(2), 166-176. https://doi.org/10.1080/15226514.2021.1929826

Win-Shwe, T., & Fujimaki, H. (2011). Nanoparticles and neurotoxicity. *International Journal of Molecular Sciences, 12*(9), 6267-6280. https://doi.org/10.3390/ijms12096267

Yang, G., Wang, Y., Wang, T., Wang, D., Weng, H., Wang, Q., & Chen, C. (2021). Variations of enzymatic activity and gene expression in zebrafish (Danio rerio) embryos Co-exposed to zearalenone and fumonisin B1. *Ecotoxicology and Environmental Safety, 222*, 112533. https://doi.org/10.1016/j.ecoenv.2021.112533

Zhang, Q., Zhang, K., Xu, D., Yang, G., Huang, H., Nie, F., Liu, C., & Yang, S. (2014). CuO nanostructures: Synthesis, characterization, growth mechanisms, fundamental properties, and applications. *Progress in Materials Science, 60*, 208-337. https://doi.org/10.1016/j.pmatsci.2013.09.003